

White cathodoluminescence from $\text{Zn}_{0.3}\text{Mg}_{0.7}\text{Al}_2\text{O}_4:\text{Tb}^{3+},\text{Eu}^{3+}$.

Shaath SKK^{1,2}, Swart HC¹ and Ntwaeaborwa OM^{1,*}

¹ Department of Physics, University of the Free State, Bloemfontein, ZA9300, South Africa.

² Department of Physics, Islamic University, P. O. Box 108, Gaza, Palestine.

* Corresponding author: ntwaeab@ufs.ac.za

Abstract. In this study, white cathodoluminescence (CL) was generated from $\text{Zn}_{0.3}\text{Mg}_{0.7}\text{Al}_2\text{O}_4:\text{Tb}^{3+};\text{Eu}^{3+}$ prepared by the combustion route using urea as a fuel metal and nitrates as precursors. The X-ray diffraction (XRD) patterns from the samples showed phases associated with cubic structures of ZnAl_2O_4 and MgAl_2O_4 . The particle morphology of the $\text{Zn}_{0.3}\text{Mg}_{0.7}\text{Al}_2\text{O}_4:\text{Tb}^{3+};\text{Eu}^{3+}$ showed different irregular shapes. White CL with the CIE coordinates ($x = 0.343$, $y = 0.323$) was observed when the phosphor was excited by a low voltage (2 keV) electron beam in vacuum. This was a result of the simultaneous emission of blue and green emissions from Tb^{3+} , and red emission from Eu^{3+} . This phosphor is evaluated for possible applications in white LEDs. .

1. Introduction

Nowadays, researchers are working to prepare, and develop white light emitting phosphors that can be used in solid state lighting applications such as flat panel displays (FPD), phosphor lamps and light emitting diodes (LEDs). The white colour is the combination of the primary colours namely blue, green and red. It is, however, not easy to have one phosphor to emit these three colours simultaneously. Traditionally, the production of white light in LEDs can be achieved by two routes. These are by combining yellow phosphor such as $\text{YAG}:\text{Ce}^{3+}$ with a InGaN -based blue diode and by combining a UV chip with a three converter system of red, green, and blue phosphors. The problems with these are poor rendition and high thermal quenching of the yellow phosphor and reabsorption of the blue emission by the red or green phosphor in the three converter system [1]. To overcome these problems, a new generation of single host phosphors prepared mostly by doping alkali earth aluminates with divalent alkali earth and/or trivalent rare-earth ions has been developed. Alkali earth aluminates are chemically stable, environmentally friendly [2], and they can be easily produced cost-effectively. For example, a white emission from a tunable $\text{Mg}_3\text{Al}_2\text{O}_5\text{Cl}_2:\text{Ce}^{3+},\text{Eu}^{2+}$ phosphor based on energy transfer from Ce^{3+} to Eu^{2+} by a down-conversion process was reported by Song et al [1], while Shaath et al [3] generated white light from $\text{Ca}_x\text{Sr}_{(1-x)}\text{Al}_2\text{O}_4:\text{Tb}^{3+};\text{Eu}^{3+}$ phosphor. In this study the combustion method was used to prepare $\text{Zn}_{0.3}\text{Mg}_{0.7}\text{Al}_2\text{O}_4:\text{Tb}^{3+};\text{Eu}^{3+}$ to produce white cathodoluminescence. The structure, morphology and cathodoluminescent (CL) properties of the prepared phosphor were examined, and are reported.

2. Experimental

2.1 Sample Preparation

A combustion method was used to prepare Tb^{3+} and Eu^{3+} co-doped $\text{Zn}_{0.3}\text{Mg}_{0.7}\text{Al}_2\text{O}_4$ nanophosphor. The metal nitrates of $\text{Zn}(\text{NO}_3)_2 \cdot 4\text{H}_2\text{O}$, $\text{Mg}(\text{NO}_3)_2 \cdot 6\text{H}_2\text{O}$, $\text{Al}(\text{NO}_3)_3 \cdot 9\text{H}_2\text{O}$, $\text{Tb}(\text{NO}_3)_3 \cdot 6\text{H}_2\text{O}$, $\text{Eu}(\text{NO}_3)_3 \cdot 5\text{H}_2\text{O}$, and urea CON_2H_4 of AR grade purchased from Merck, South Africa were used as starting materials (precursors), and were used as obtained without further purification. Distilled water was used to dissolve the precursors with vigorous stirring at 50°C for 0.3 hr until the solution became clear. The resulting solution was transferred to a muffle furnace maintained at $450 \pm 10\%$ °C. The

transparent solution started to boil, and underwent dehydration, followed by decomposition, and escaping of large amounts of gases (nitrogen, ammonia and oxides of carbon). White foamy, and voluminous ash was produced after an occurrence of spontaneous ignition, and the reaction underwent smouldering combustion with enormous swelling. The combustion reaction was completed in ~5 minutes. The product was cooled to room temperature, and the ashes were ground gently into fine powders. The powders were characterized without any further post-preparation treatment. The crystalline structure of $\text{Zn}_{0.3}\text{Mg}_{0.7}\text{Al}_2\text{O}_4:\text{Tb}^{3+};\text{Eu}^{3+}$ was analysed with a Bruker D8 ADVANCE powder X-ray diffractometer (XRD) with Cu $K\alpha$ radiation, $\lambda=1.5406 \text{ \AA}$. The scanning electron microscopy (SEM) data were collected with a JEOL-JSM 7500 Scanning Electron microscope operated at 30 Kv, and 50 pA. The CL emission spectra were measured for using a beam of 2 keV, and 400 μA emission current as excitation source. All measurements were carried out at room temperature.

3. Analysis and results discussion

3.1. Structural analyses.

MgAl_2O_4 and ZnAl_2O_4 materials belong to a close-packed spinel cubic structure with O_h^7 (Fd3m) space group symmetry [4-10]. The general chemical formula for the spinel structure is given by (1)



where X and Y are the cations with valence number (2+) and (3+), respectively, and the concentration of X and Y that fill the tetrahedral site $()_{\text{Tet.}}$ and octahedral site $\{ \}_{\text{Oct.}}$ is much equal to or less than 1. The normal spinel is obtained when $s=0$ (i.e. XY_2O_4) with eight formula units per cubic unit cell [9], otherwise an intermediate or distorted spinel is obtained. Therefore, according to the formula (1) the divalent ions Mg^{2+} and/or Zn^{2+} can be distributed into the tetrahedral and octahedral sites, and the same for Al^{3+} . This is in agreement with the network connection of MgAl_2O_4 shown in Fig. 1 [11]. It appears in the given structure that there are two positions for Mg^{2+} and Al^{3+} i.e. (Mg1 and Al2) and (Mg2 and Al1). It looks like that there is no effect or change when Zn^{2+} ions are added to the MgAl_2O_4 by small amount because the Mg^{2+} (ionic radius = 0.051 nm) and Zn^{2+} (ionic radius = 0.074 nm) have almost the same ionic radii [12], and have the same valency. Therefore, Zn^{2+} can occupy the two different sites of Mg^{2+} with ease. In addition, Tb^{3+} (ionic radius = 0.106 nm), and Eu^{3+} (ionic radius = 0.109 nm) ions can replace cations Al^{3+} (ionic radius = 0.053 A°) and/or Mg^{2+} , and/or Zn^{2+} [12], or they can stay on the surface of the host lattice, the latter possibility is more appropriate because the ionic radii of the dopants are larger than those of the cations [13]. Fig. 2 presents the XRD patterns of $\text{Zn}_{0.3}\text{Mg}_{0.7}\text{Al}_2\text{O}_4:\text{Tb}^{3+},\text{Eu}^{3+}$. The pattern is consistent with the standard cubic structure of MgAl_2O_4 referenced in JCPDS file No. 75-1796. This indicates that, a pure single phase spinel cubic structure of $\text{Zn}_{0.3}\text{Mg}_{0.7}\text{Al}_2\text{O}_4:\text{Tb}^{3+},\text{Eu}^{3+}$ was crystallized. This is due to the fact that both MgAl_2O_4 and ZnAl_2O_4 have the same cubic spinel structure, and have the same diffraction peaks. The average particle size estimated using the Debye-Scherrer formula was ~22 nm. The lattice parameters of $\text{Zn}_{0.3}\text{Mg}_{0.7}\text{Al}_2\text{O}_4:\text{Tb}^{3+},\text{Eu}^{3+}$ were calculated, and are given in Table 1, and they compare very well with the standard parameters referenced in JCPDS file No. 75-1796.

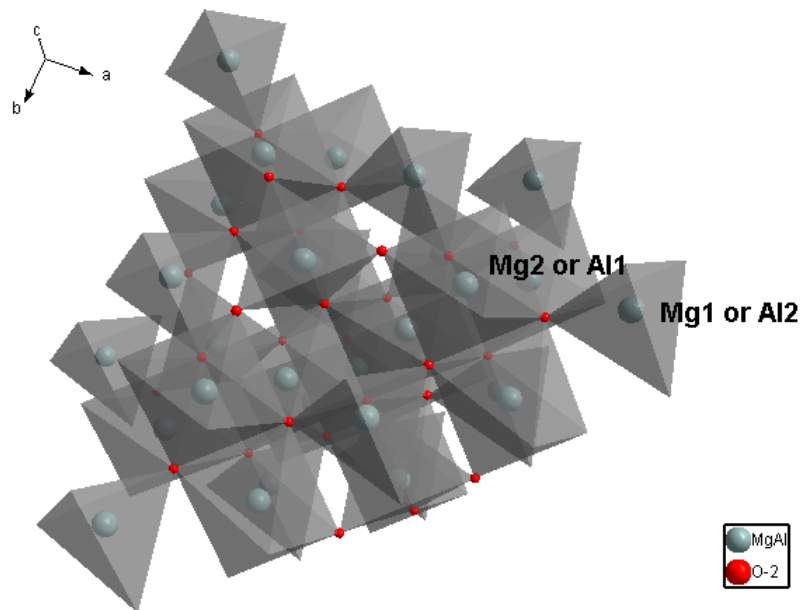


Fig. 1: The connection of the network of atoms in MgAl_2O_4 [11].

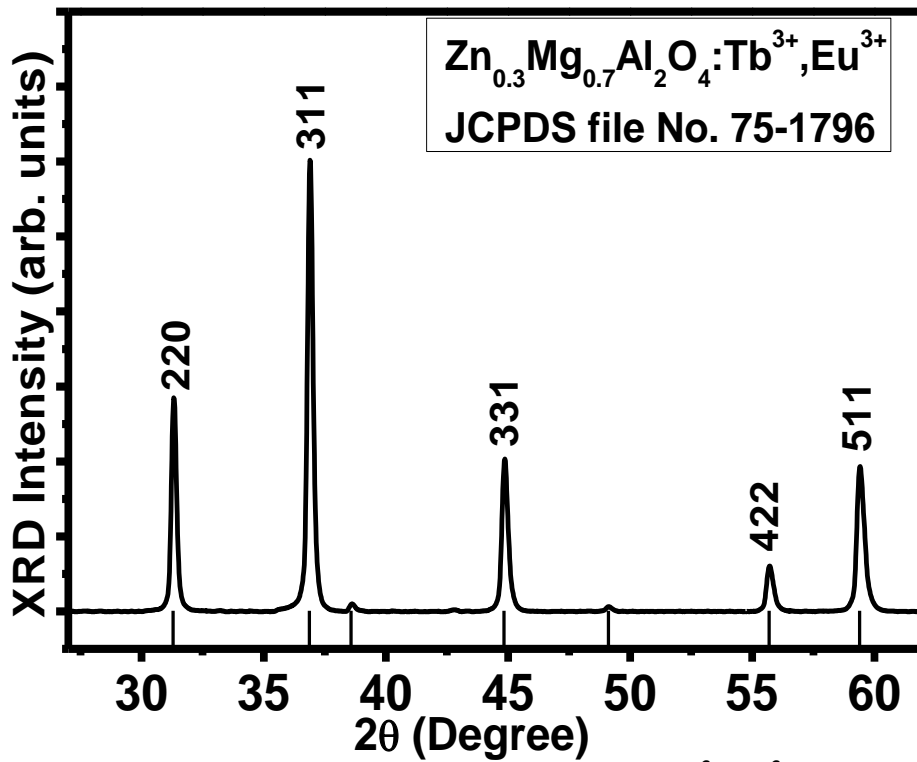


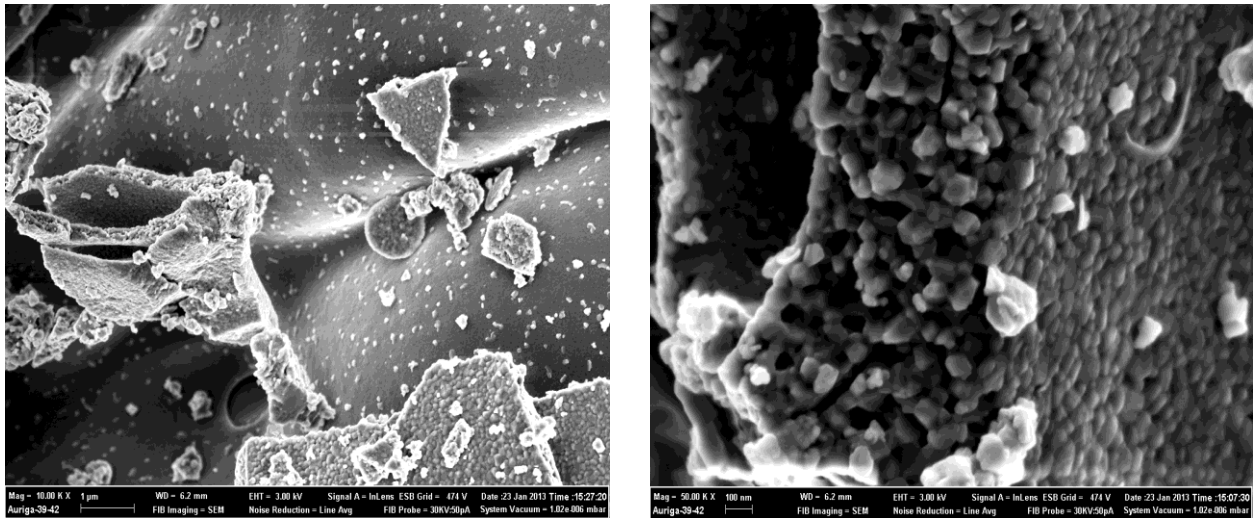
Fig. 2: XRD patterns of $\text{Zn}_{0.3}\text{Mg}_{0.7}\text{Al}_2\text{O}_4:\text{Tb}^{3+},\text{Eu}^{3+}$.

Table 1: Lattice parameters of $\text{Zn}_{0.3}\text{Mg}_{0.7}\text{Al}_2\text{O}_4:\text{Tb}^{3+},\text{Eu}^{3+}$.

	Lattice constants			Angles		
	A	b	c	α	Γ	β
$\text{Zn}_{0.3}\text{Mg}_{0.7}\text{Al}_2\text{O}_4:\text{Tb}^{3+},\text{Eu}^{3+}$.	8.07Å	8.07Å	8.07Å	90°	90°	90°
JCPDS file No. 75-1796.	8.70Å	8.70Å	8.70Å	90°	90°	90°

3.2. Morphology study.

The particle morphology of the $\text{Zn}_{0.3}\text{Mg}_{0.7}\text{Al}_2\text{O}_4:\text{Tb}^{3+},\text{Eu}^{3+}$ powders are shown in Fig. 3. The well-known semicontinuous folded dense platelet like morphology was observed, and there were also voids resulting from evolution, and escape of large amount of gases during the combustion process. Notice that the platelets were encrusted with smaller spherical particles.

**Fig. 3: SEM images for the $\text{Zn}_{0.3}\text{Mg}_{0.7}\text{Al}_2\text{O}_4:\text{Tb}^{3+},\text{Eu}^{3+}$.**

3.3. Cathodoluminescence study.

Fig. 4 shows the CL emission spectrum of the $\text{Zn}_{0.3}\text{Mg}_{0.7}\text{Al}_2\text{O}_4:\text{Tb}^{3+},\text{Eu}^{3+}$ recorded when the phosphor was bombarded with a low-voltage electron beam at 2 keV. As shown in Fig. 4, the CL spectrum consists of blue, green, and red emission arising from Tb^{3+} and Eu^{3+} transitions. The blue emissions at 381, 418, and 438 nm are ascribed to $^5\text{D}_3 \rightarrow ^7\text{F}_j$ ($J=6,5,4,3,2,1$, and 0) transitions of Tb^{3+} , the green emissions at 473, 491 and 547 nm are attributed to $^5\text{D}_4 \rightarrow ^7\text{F}_j$ ($J=6,5,4,3,2,1$ and 0) transitions of Tb^{3+} [14], and red emissions at 594, 619, 655, and 705 nm are ascribed to $^5\text{D}_0 \rightarrow ^7\text{F}_j$ ($J=0,1,2,3,4,5$ and 6) transitions of Eu^{3+} [14]. Among the Eu^{3+} transitions, the most intense emission peak at 619 nm, corresponding to $^5\text{D}_0 \rightarrow ^7\text{F}_2$, usually occurs through the electric dipole transition (EDT), while the $^5\text{D}_0 \rightarrow ^7\text{F}_1$ band at 594 nm is the magnetic dipole transition (MDT) [13]. The intensity of this transition increased with a decreasing local symmetry of the Eu^{3+} ion [15]. The CL emission spectra of $\text{Zn}_{0.3}\text{Mg}_{0.7}\text{Al}_2\text{O}_4:\text{Tb}^{3+},\text{Eu}^{3+}$ suggest that there is no energy transfer between Tb^{3+} and Eu^{3+} since the blue, green and red emissions occurred simultaneously. Fig. 5 shows the calculated CIE-1931 chromaticity coordinates diagram of white emissions from $\text{Zn}_{0.3}\text{Mg}_{0.7}\text{Al}_2\text{O}_4:\text{Tb}^{3+},\text{Eu}^{3+}$ obtained by CL excitation. The chromaticity coordinates of the white light are $x = 0.342$, $y = 0.323$, and are very close to the chromaticity coordinates of standard white light CIE-E ($x = 0.333$, $y = 0.333$) [16].

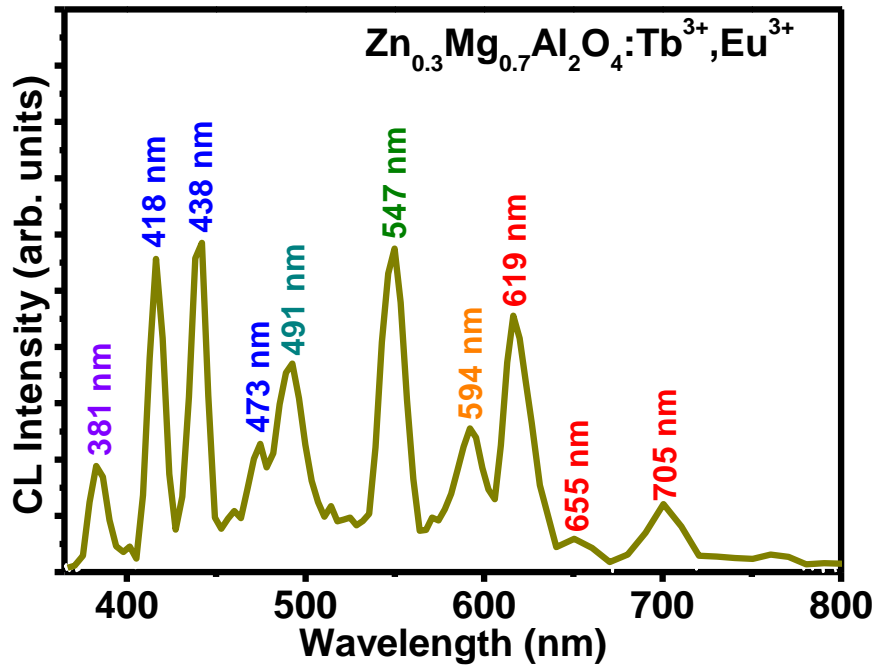


Fig. 4: CL emission spectra of $\text{Zn}_{0.3}\text{Mg}_{0.7}\text{Al}_2\text{O}_4:\text{Tb}^{3+},\text{Eu}^{3+}$.

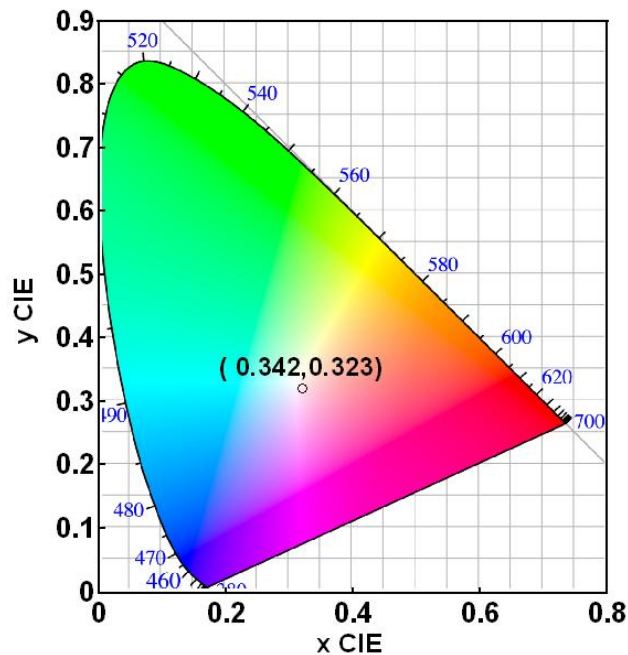


Fig. 5: The CIE diagram showing coordinates of $\text{Zn}_{0.3}\text{Mg}_{0.7}\text{Al}_2\text{O}_4:\text{Tb}^{3+},\text{Eu}^{3+}$.

4. Conclusion

White cathodoluminescence was observed from $\text{Zn}_{0.3}\text{Mg}_{0.7}\text{Al}_2\text{O}_4:\text{Tb}^{3+},\text{Eu}^{3+}$. The structure resembles a single phase cubic structure. The white generated light was the result of the combination of blue and green narrow line emission from Tb^{3+} and the red emission from Eu^{3+} . This phosphor holds good prospects for application in solid state lighting.

Acknowledgement

The authors would like to acknowledge the financial support from the cluster funds of the University of the Free State, the South African National Research Foundation (NRF), the South African National Laser centre (NLC), and the South African Research Chairs Initiative of the Department of Science and Technology and National Research Foundation of South Africa.

References

- [1] Song Y, Jia G, Yang M, Huang Y, You H and Zhang H 2009 *Appl. Phys. Lett.* **94** 091902.
- [2] Mothudi B, Ntwaeaborwa M, Pitale S and Swart H 2010 *J. Alloys Compd.* **508** 262.
- [3] Shaat S, Swart H and Ntwaeaborwa M 2012 *Opt. Mater. Express* **7** 962.
- [4] Hernandez-Perez C, Garcia-Hipolito M, Alvarez-Perez M, Alvarez-Fregoso O, Ramos-Brito F and Falcony C 2010 *Phys. Status Solidi A* **207** 417.
- [5] Miron I, Enache C, Vasile M and Grozescu I 2012 *Phys. Scr. T.* **149** 014064.
- [6] Zawrah M, Hamaad H and Meky S 2007 *Ceram. Int.* **33** 969.
- [7] Wiglusz R, Grzyb T, Lis S and Strek W 2010 *J. Lumin.* **130** 434.
- [8] Sanjeev M, Bhushan D, Alagu R, Morea S, Gundu T and Khera R 2008 *J. Lumin.* **128** 1673.
- [9] Nakagawaa H, Ebisua K, Zhanga M and Kitaura M 2003 *J. Lumin.* **102** 590.
- [10] Yutaka F, Hiroaki T, Kazuhiro I, Shigetomo Y, Shiori M, Masanobu S, Kouichirou T, Yutaka K and Eiichi H 2008 *J. Lumin.* **128** 282.
- [11] Diamond, Version 3.0d, 1997–2005 Copyright© Crystal Impact GbR, Bonn, Germany.
- [12] Magnesium, [online], Available from <http://www.webelements.com/magnesium/> [Accessed at 22 Feb 2013].
- [13] Xiang Y and Chao M 2010 *Opt. Mater.* **32** 415.
- [14] Dongling G, Guogang L, Mengmeng S, Chong P, Yang Z, Ziyong C and Jun L 2012 *Dalton Trans.* **41** 3078.
- [15] Yufeng C, Songhua Z, Fei L, Fan L and Yiwang C 2011 *J. Lumin.* **131** 701.
- [16] Fan S, Yu C, He D, Wang X and Hu L 2012 *Opt. Mater. Express* **2(6)** 765.